
Diffuse layers on the surface of mineral quartz

Matthew C. Ball, David S. Brown and Louise J. Perkins

Department of Chemistry, Loughborough University, Loughborough, Leicester, UK LE11 3TU

The effect of simple chemical and physical treatments on the formation of a diffuse layer on the surface of a mineral quartz has been studied by small-angle X-ray scattering. The changes in layer thickness are related to changes in surface composition as determined by ESCA.

Silica, in the form of crystalline quartz and in many gel formulations, is important commercially. The high surface area materials are used as fillers, catalyst supports and as thickening and extending agents in liquids.¹ Naturally occurring quartz is used in slightly different ways, largely on the grounds of cost: as a supposedly inert filler in cements and mortars, in resin and clay-bonded sand moulds in the metal casting industry,² and in other polymer-bonded composites, as an abrasive (sand paper). In all of these uses the interface properties between the silica and other phases are important.

The reactivity of silica surfaces has been studied extensively, and the literature up to 1976 has been summarized well by Iler.³ Most of the work described is concerned with the properties of pure silica in its various forms, and Iler highlights two aspects of the surface chemistry which are relevant to the present work. The first is the chemistry of the surface —Si—OH groups (including geminal and vicinal groups) and their reactivity towards other molecules. Such reactivity arises mainly through hydrogen bonding, but acid–base reactions also occur. The number of —Si—OH groups is dependent on the surface area of the silica and on temperature. The second point discussed by Iler is the formation of an amorphous or disturbed layer at the silica surface. Recently such layers have been held responsible for anomalous solubility determinations for quartz,^{4,5} although there is no general agreement on their occurrence.⁶ The measurement of solubility is complicated by the sorption of cations from solution which slows the rate of dissolution. The formation and properties of such amorphous layers on quartz have been studied by Ritchie and co-workers,⁷ and also by Alexanian.⁸ The formation of an amorphous layer by grinding⁹ and pulverising under water¹⁰ have also been examined. The surface chemistry of crystalline quartz will be modified by the presence of such layers.

The gel materials studied previously were of relatively high purity (SiO₂ = 99+ % on an ignited basis) with the main impurity species being alkali metals, with small amounts of calcium, magnesium, iron and aluminium. There is some evidence that the impurities increase the sorptive capacity of these gels,¹¹ and therefore that impurities might be present at the surface. It is generally assumed that the crystalline materials have the same surface chemistry as the gels.¹²

Two grades of quartz sands are commercially available: those of high purity (99.8+ % SiO₂), on which most of the work mentioned above was carried out, and the much more common and cheaper grades (96% SiO₂), with Al, Fe, *etc.*, making up the balance. Little work has been done to study either the distribution of these impurities or their effects on the acid–base chemistry and the amorphous layers.

Experimental

Material

The raw material was a natural quartz flour supplied by British Industrial Sands Ltd. (Cauldon, Derbyshire). SEM examin-

ation showed that approximately 75% of the particles had diameters around 1 μm , with the range extending between 10 and 0.1 μm . No compounds other than quartz could be detected by XRD in this material.

Instrumental techniques

X-Ray fluorescence (XRF). The equipment used was a Phillips PW 1480 XRF spectrometer, using a scandium–molybdenum alloy source.

Electron spectroscopy (ESCA). The spectrometer used was an Escalab 5 electron spectrometer (Vacuum Generators Ltd.) using either Al-K α (1486.6 eV) or Mg-K α (1254.4 eV) radiation and a pass energy of 15 eV. Chemical shifts were also measured by using the carbon peak at 284.7 eV: this peak was always present. Inorganic carbon as carbonate was always looked for in high resolution scans. Derived sensitivity factors were used to convert signal intensities into concentrations.¹³

Small-angle X-ray scattering (SAXS). A Rigaku-Denki small-angle spectrometer using Cu-K α radiation ($\lambda = 1.5418 \text{ \AA}$) and slit optics was used to determine the X-ray scattering over the angular range $2\theta = 0.5\text{--}2.5^\circ$ in steps of 0.02° with a counting time of 1000 s. The sample was mounted as a thin layer between Mylar film, using an aluminium holder with a 0.02 cm spacer. Backgrounds were measured under the same conditions with the sample in an absorbing position and subtracted from the sample-scattered intensities. The resulting data were smoothed by Savitzky–Golay moving-window methods.

XRD, SEM and DRIFT studies and surface area determinations were also undertaken.

Sample treatments. Simple treatments were used to modify the sand surface: water washing used repeat volumes of distilled water, with vigorous shaking, until all fine particles were removed and the supernatant liquid did not leave a residue on evaporation. The fine particles, on examination by XRD, were shown to be quartz also. Acid treatment of the washed material was with 1 mol dm⁻³ hydrochloric acid over time; samples were then shaken with distilled water until the washings were neutral. Samples of washed quartz were heated at various temperatures up to 1523 K.

Results

Physical effects of treatment—diffuse layer thickness

Porod's law¹⁴ indicates that a plot of $\ln I$ vs. $\ln 2\theta$ for a perfect two-phase system should have a slope of -3.0 (for the infinite slit geometry used); I = intensity of scattered radiation and 2θ = scattering angle. Negative deviations from Porod's law indicate a surface layer of lower density than the bulk, while positive deviations indicate bulk density variations. Fig. 1 and

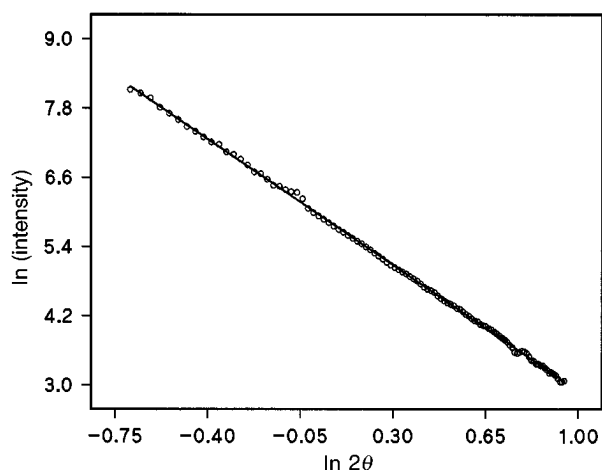


Fig. 1 $\ln I$ vs. $\ln 2\theta$ for as-received sand

2 show such plots for the as-received sand and for the sand heated at 1250 K. The difference in slope between the two below $\ln 2\theta = 0.5$ is obvious. Statistical data for these two plots are included in Table 1.

The thickness of the diffuse layer (δ) can be estimated from an empirical approach based on a plot of $\ln(s^3 I)$ vs. $s^{1.81}$ (where $s = 2\sin\theta/\lambda$) for the range of data showing the negative deviation, assuming that the change in density is sigmoidal:¹⁵

$$s^3 I = k \exp[-38(\sigma s)^{1.81}]; \sigma = (-\text{slope}/38)^{1/1.81}$$

where σ is the diffuse layer thickness parameter and $\delta = \sqrt{12}\sigma$. This expression applies to infinite slit geometry.

Fig. 3 and 4 show such plots derived from scattering from the two samples compared in Fig. 1 and 2. Derived data from these are included in Table 1, where the differences in slope for the high-angle data are quantified.

Table 2 shows the diffuse layer thickness calculated from the small-angle X-ray scattering data for various samples. Only the original material and that heated to 1523 K show no

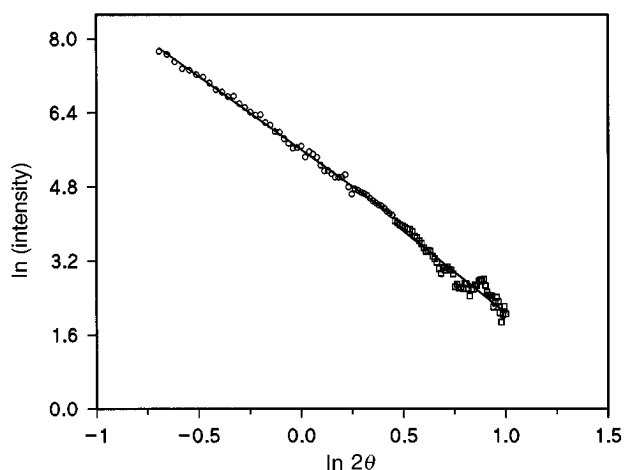


Fig. 2 $\ln I$ vs. $\ln 2\theta$ for sand heated to 1273 K

Table 1 Statistical data for the plots shown in Fig. 1 and 2

sample	$\ln I$ vs. $\ln 2\theta$				$\ln s^3 I$ vs. $s^{1.81}$	
	$2\theta < 0.5$		$2\theta > 0.5$		slope	r
	slope	r	slope	r		
as-received sand	-2.99	0.9967	-2.99	0.9967	-183.7	-0.6630
heated at 1273 K	-3.17	0.9983	-3.54	0.9660	-396.8	-0.8447

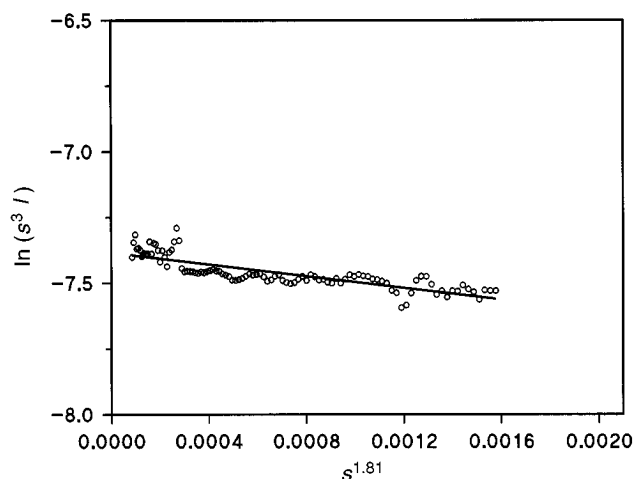


Fig. 3 Diffuse layer plot for as-received sand

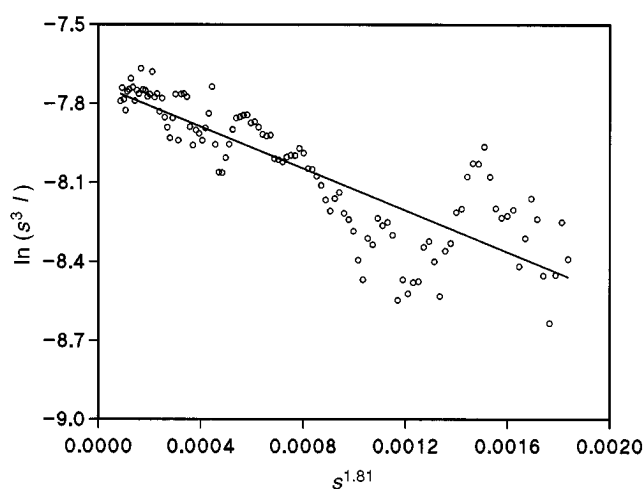


Fig. 4 Diffuse layer plot for sand heated to 1273 K

Table 2 Gradients from Porod's law plots

sample	slope of plot	δ/pm
as-received	-2.99	0
acid:		
1 mol dm ⁻³ , 24 h	-3.22	200
1 mol dm ⁻³ , 48 h	-3.19	400
1 mol dm ⁻³ , 144 h	-3.37	1300
heated to:		
1000 K	-3.27	900
1273 K	-3.54	1800
1523 K	-2.98	0

significant deviations from Porod's law, and therefore have either a very thin diffuse layer or none. The diffuse layer thickness increases with time and with temperature for acid and heat treatments respectively. The disappearance of the layer at 1523 K is in line with the sintering observed in this sample: clearly, the surface layer of the material is becoming very mobile.

Chemical effects of treatment—surface analysis

Starting material. Analytical results for the as-received and treated sands are given in Table 3. These are expressed analytically as atom% and have been re-calculated to exclude carbon which was shown to be only aliphatic. These corrected atom contents have been converted to oxide contents in Table 4, and show that the sand is comparatively pure in bulk terms (96.9% SiO₂) and that the major bulk impurities are aluminium

Table 3 ESCA analyses of quartz flour

treatment	Si	Al	Fe	Mg	Ca	K	Na	O	C
including carbon:									
as received	21.2	6.5	0.9	4.4	0.9	—	—	39.0	27.1
water wash	21.4	6.5	1.0	2.6	0.9	0.4	—	46.7	20.4
acid wash: 48 h	22.5	6.3	0.9	2.5	0.6	0.5	—	48.6	18.2
144 h	24.4	4.4	0.8	1.8	0.5	0.7	—	51.0	16.3
heat-treated	24.7	7.0	—	1.5	—	0.9	—	46.6	19.2
excluding carbon:									
as received	29.1	8.9	1.0	6.0	1.2	—	—	53.9	
water wash	26.9	8.2	1.3	3.3	1.1	0.5	—	58.7	
acid wash: 48 h	27.5	7.7	1.1	3.0	0.7	0.6	—	59.4	
144 h	29.1	5.3	1.0	2.2	0.6	0.8	—	61.0	
heat-treated	30.6	8.7	—	1.9	—	1.1	—	57.7	

(1.6%), potassium (1%) and iron (0.2%). It is interesting that these impurities are the same as those found in the synthetic gel materials. The surface analysis, on the other hand, shows that the impurity species are concentrated at the sand surface, to such an extent that the SiO₂ content is reduced to <70%, with aluminium being concentrated eleven-fold, iron ten-fold, and calcium twenty-fold over the bulk values. Magnesium does not appear in the bulk analysis but makes up approximately 10% of the surface, so that the surface enrichment for this element is very high.

Treated materials. Washing of the sand causes a reduction in the bulk potassium, but a slight increase in surface potassium. The surface iron and calcium contents also increase on washing. Magnesium levels are halved on washing, but it still makes up nearly 6% of the surface.

Acid washing removes aluminium, magnesium and calcium and, to a lesser extent, iron.

Heating reduces the iron content of the surface, until at 1523 K no iron was detectable. Magnesium and calcium were also depleted at high temperature.

Other effects of treatment

Surface area determination. Surface areas as measured by nitrogen sorption gave a value for the starting material of 1.36 m² g⁻¹. This value increased a little with 144 h of acid treatment to 1.61 m² g⁻¹. Heat treatment to 1273 K produced no change, while heating at 1523 K reduced the area to 0.17 m² g⁻¹.

SEM examination. No great differences between samples were apparent from SEM examination.

IR spectroscopy. DRIFT spectroscopy shows very little difference between the spectra of any of the samples, irrespective of treatment. It is interesting that little or no change in absorption occurs in the water/hydroxy region near 3400 cm⁻¹.

Discussion

Surface impurities such as those identified here could be caused by the presence of adhering minerals, particularly clay or feldspar, or species present in solid solution in the quartz. No extraneous minerals were detected by XRD, however. Washing with water would be expected to remove at least some of the former, while both would be susceptible to acid attack or heat.

As-received and washed sand

The original material has a high concentration of aluminium at the surface, and this is enriched by the same factor as iron, present at much lower concentration. The high surface concentration of magnesium appears unexpected, but similar

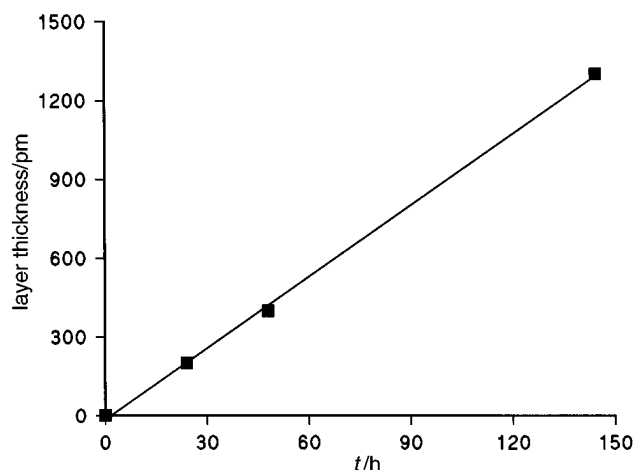


Fig. 5 Diffuse layer thickness from acid treatment vs. time

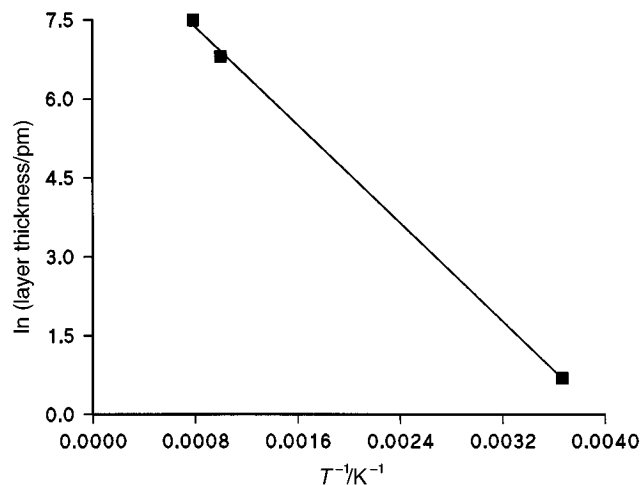


Fig. 6 Arrhenius plot for diffuse layer thickness vs. temperature

Table 4 Bulk (XRF) and surface (ESCA) analyses of quartz flour

treatment		oxide composition (mass%)								
		SiO ₂	Al ₂ O ₃	Fe ₂ O ₃	MgO	CaO	K ₂ O	Na ₂ O	TiO ₂	
as received	XRF	96.9	1.6	0.2	—	0.1	1.0	0.1	—	
	ESCA	69.0	17.6	2.0	9.5	1.9	—	—	—	
water wash	XRF	98.1	1.5	0.2	—	0.1	—	—	0.1	
	ESCA	68.7	17.7	4.4	5.6	2.6	1.0	—	—	
acid wash: 48 h	XRF	98.1	1.6	0.1	—	0.1	—	—	0.1	
	ESCA	71.1	17.0	3.5	5.3	1.2	1.8	—	—	
	144 h	XRF	98.1	1.6	0.1	—	0.1	—	—	0.1
		ESCA	77.4	12.0	3.5	3.9	1.5	1.7	—	—
heat (1523 K)	XRF	97.9	1.7	0.2	—	0.1	—	—	0.1	
	ESCA	77.1	18.3	—	3.2	—	1.4	—	—	

enrichments have been found in synthetic silicates¹⁶ and commercial cements.¹⁷ Washing makes relatively little difference, except to increase the amount of iron and potassium at the surface, and to reduce the bulk potassium. This could be caused by dissolution of the potassium, followed by spreading across the surface. The diffuse layer is either very thin or non-existent in both samples.

Acid treatment

Most surface cations are attacked by acid, as has been noted previously.¹⁸ This cation dissolution is associated with the linear increase in diffuse layer thickness (see Fig. 3). Zero-order kinetics are therefore followed. In most cases such behaviour would relate to reaction taking place across a constant surface area; the measured area is increasing slightly, but the increase is so small as not to distort the simple plot shown in Fig. 5. None of the treatments used seem to generate more of a hydroxy group layer than is present on the starting material, so far as can be detected by IR spectroscopy; this may be because of the relatively large sampling depth of IR studies. The changes in diffuse layer thickness are more probably related to the formation of a layer of different density than a hydroxylated layer.

Heat treatment

Heat treatment results in reduction of iron, calcium and magnesium at the surface. This is associated with an increase in the diffuse layer thickness, which disappears as the material sinters at the highest temperatures studied. It is likely that this reduction is associated with diffusion of cations into the bulk of the quartz. This suggestion is reinforced by Fig. 6. The layer thickness is logarithmic with reciprocal temperature, which suggests a thermally activated process, for which the calculated activation energy is close to 11 kJ with $A = 1.3 \times 10^4 \text{ s}^{-1}$, both of which are compatible with a diffusion process.¹⁹

We feel that an important indicator is the constancy of the aluminium at the surface. It does not behave like the other cations, reducing in concentration as a result of most processes, so it is likely that it is involved structurally in producing the surface layer. Various structures²⁰ exist which have silicon substituted by aluminium. These include the 'stuffed silica' series having the quartz, cristobalite and trydimite structures;

eukriptite, $\text{Li}(\text{AlSiO}_4)$, has the quartz structure, and kalsilite, $\text{K}(\text{AlSiO}_4)$, has the trydimite structure. Clearly these have $\text{Si}/\text{Al} = 1.0$. Feldspars, with $\text{Si}/\text{Al} = 1.0$ or 2.0, exist in a wide range of structures, while the zeolites have Si/Al substitution ratios between 1.0 and 5.5 (mordenite). Ultramarines have an Si/Al ratio of 2.0. The Si/Al ratio is 3.52 for the heated sand, which is higher than most of the perfect structural values given above, but less than the value for mordenite, which is a zeolite with twelve silicate tetrahedra in the ring. The formation of such structures at the surface would lead to a reduction in density.

References

- 1 P. Kleinschmit, in *Speciality Inorganic Chemicals*, ed. R. Thompson, Royal Society of Chemistry, London, 1981.
- 2 See, for example, *Clay-bonded Foundry Sands*, W. B. Parkes, Applied Science Publishers, London, 1971.
- 3 R. K. Iler, *The Chemistry of Silica*, John Wiley, New York, 1979.
- 4 J. D. Rimstead and H. L. Barnes, *Geochim. Cosmochim. Acta*, 1980, **44**, 1683.
- 5 R. Wollast and L. Chou, *Trans. XIII Congress of the ISSS*, ISSS, Hamburg, 1986, p. 127.
- 6 W. A. House and D. R. Orr, *J. Chem. Soc., Faraday Trans.*, 1992, **88**, 233.
- 7 See the series of papers which ends with J. Brown, W. J. Jaap and P. D. Ritchie, *J. Appl. Chem.*, 1959, **9**, 153.
- 8 C. R. Alexanian, *C. R. Acad. Sci.*, 1956, **242**, 2145.
- 9 M. S. Patterson and K. Wheatley, *J. Appl. Chem.*, 1959, **9**, 231.
- 10 L. G. Ganischenko, M. M. Egorov, V. F. Kiselev, K. G. Krasil'nikov and G. S. Khodakova, *Dokl. Akad. Nauk SSSR*, 1960, **131**, 597.
- 11 J. A. Hockey and B. A. Pethica, *Trans. Faraday Soc.*, 1961, **57**, 2247.
- 12 J. A. Hockey, *Chem. Ind.*, 1965, **9**, 57.
- 13 J. T. Grant, *Surf. Sci. Anal.*, 1989, **14**, 271.
- 14 G. Porod, *Kolloid-Z.*, 1952, **125**, 108.
- 15 J. T. Korberstein, B. Morra and R. S. Stein, *J. Appl. Crystallogr.*, 1980, **13**, 34.
- 16 M. C. Ball and I. Sutherland, *J. Mater. Chem.*, 1995, **5**, 1459.
- 17 M. C. Ball, R. E. Simmons and I. Sutherland, *Cem. Conc. Res.*, 1988, **18**, 29.
- 18 J. G. Gibb and P. D. Ritchie, *J. Appl. Chem.*, 1954, **4**, 473.
- 19 H. F. Cordes, *J. Phys. Chem.*, 1968, **72**, 2185.
- 20 A. F. Wells, *Structural Inorganic Chemistry*, OUP, Oxford, 3rd edn., 1962, ch. 21; L. Smart and E. Moore, *Solid State Chemistry*, Chapman and Hall, London, 1992, ch. 5.

Paper 6/03570A; Received 22nd May, 1996